Icarus 252 (2015) 327–333

Contents lists available at ScienceDirect

Icarus

journal homepage: www.elsevier.com/locate/icarus

Vertical profiles of H_2O, H_2SO_4, and sulfuric acid concentration at 45–75 km on Venus

Vladimir A. Krasnopolsky *

Department of Physics, Catholic University of America, Washington, DC 20064, USA
Moscow Institute of Physics and Technology (PhysTech), Dolgoprudny, Russia

ARTICLE INFO

Article history:
Received 5 December 2014
Revised 27 January 2015
Accepted 29 January 2015
Available online 13 February 2015

Keywords:
Venus
Venus, atmosphere
Atmospheres, composition
Atmospheres, chemistry
Abundances, atmospheres

ABSTRACT

A method developed by Krasnopolsky and Pollack (Krasnopolsky, V.A., Pollack, J.B. [1994]. Icarus 109, 58–78) to model vertical profiles of H_2O and H_2SO_4 vapors and sulfuric acid concentration in the Venus cloud layer has been updated with improved thermodynamic parameters for H_2O and H_2SO_4 and reduced photochemical production of sulfuric acid. The model is applied to the global-mean conditions and those at the low latitudes and at 60°. Variations in eddy diffusion near the lower cloud boundary are used to simulate variability in the cloud properties and abundances of H_2O and H_2SO_4. The best version of the model for the global-mean condition results in a lower cloud boundary (LCB) at 47.5 km, H_2SO_4 peak abundance of 7.5 ppm at the LCB, and H_2O mixing ratios of 7 ppm at 62 km and 3.5 ppm above 67 km. The model for low latitudes gives LCB at 48.5 km, the H_2SO_4 peak of 5 ppm, H_2O of 8.5 ppm at 62 km and 3 ppm above 67 km. The model for 60° shows LCB at 46 km, the H_2SO_4 peak of 8.5 ppm, H_2O of 9 ppm at 62 km and 4.5 ppm above 67 km. The calculated variability is induced by the proper changes in the production of sulfuric acid (by factors of 1.2 and 0.7 for the low latitudes and 60°, respectively) and reduction of eddy diffusion near 45 km relative to the value at 54 km by factors of 1.1, 3, and 4.5 for the low and middle (global-mean) latitudes and 60°, respectively. Concentration of sulfuric acid at the low and middle latitudes varies from ~98% near 50 km to ~80% at 60 km and then is almost constant at 79% at 70 km. Concentration at 60° is 98% at 50 km, 73% at 63 km, and 81% at 70 km. There is a reasonable agreement between the model results and observations except for the sulfuric acid concentration in the lower clouds. Variations of eddy diffusion in the lower cloud layer simulate variations in atmospheric dynamics and may induce strong variations in water vapor near the cloud tops. Variations in temperature may affect abundances of the H_2O and H_2SO_4 vapors as well.

1. Introduction

Formation of the dense and extended sulfuric acid clouds is the main feature of photochemistry on Venus. These clouds are among basic topics to study on the planet. Phase exchange between the vapors of H_2O and H_2SO_4 and the sulfuric acid droplets significantly complicates the traditional gas-phase photochemistry. Krasnopolsky and Parshev (1981, 1983) found an approximation to this problem in their photochemical model. However, later photochemical models by Yung and DeMore (1982), Mills and Allen (2007), and Zhang et al. (2012) avoided the phase exchange and adopted vertical profiles of H_2O for their calculations.

A detailed study of the phase exchange of H_2O and H_2SO_4 was made by Krasnopolsky and Pollack (1994, Paper 1), who calculated vertical profiles of H_2O, H_2SO_4, and the acid concentration from the lower cloud boundary to 65 km for two models with H_2O mixing ratios of 30 and 90 ppm in the lower atmosphere. A similar problem was solved by Krasnopolsky (2011, Paper 2) for the altitude range of 70–110 km using H_2O vertical profiles that were retrieved by Fedorova et al. (2008) from the SOIR solar occultations at Venus Express. Krasnopolsky (2012) developed a photochemical model for 47–112 km that included a calculated H_2O profile assuming that sulfuric acid is formed as $H_2SO_4 \cdot H_2O$.

While the ideas and approach in Paper I remain valid, some input data have to be updated, thus affecting the final results. This is a goal of the current paper. We will also compare the calculated profiles of H_2O, H_2SO_4, and sulfuric acid concentration at 45–75 km with some recent observational data.

Recently Gao et al. (2014) developed a model of formation of the sulfuric acid aerosol on Venus and its size distribution at various altitudes and conditions. They adopted an H_2O profile and

* Address: Department of Physics, Catholic University of America, Washington, DC 20064, USA.

http://dx.doi.org/10.1016/j.icarus.2015.01.024
0019-1035/

therefore fixed an H_2SO_4 profile and sulfuric acid concentration in their model. Their goals are very different from ours: we will not deal with the aerosol size distribution but will calculate H_2O and H_2SO_4 vapor profiles and sulfuric acid concentration as well as their variations with latitude.

2. Model

2.1. Thermodynamic data

Here we will repeat some relationships from Papers 1 and 2. Partial vapor pressures of H_2O and H_2SO_4 in phase equilibrium with liquid or solid sulfuric acid are equal to

$$\ln p_i = \ln p_{si} + \frac{\mu_i - \mu_i^0}{RT} \quad (1)$$

The subscripts $i = 0$ and 1 refer to H_2O and H_2SO_4, respectively, the subscript s means saturated vapor above a pure liquid or solid species, R is the gas constant, T is temperature, and $\mu_i - \mu_i{}^0$ is the difference of chemical potentials of a species in solution and a pure species. Chemical potentials of H_2O and H_2SO_4 in sulfuric acid for various $m = H_2O/H_2SO_4$ in the solution were tabulated by Giauque et al. (1960). The saturated H_2O pressure over ice is

$$\ln p_{s0}(\text{bar}) = -1.96250 - 5723.265/T + 3.53068 \ln T - 0.00728332T \quad (2)$$

(Murphy and Koop, 2005) and

$$\ln p_{s0}(\text{bar}) = 11.9516 - \frac{3984.93}{T - 39.7} \quad (3)$$

over liquid water at $T = 273$–373 K (http://ddbonline.ddbst.de/AntoineCalculation/AntoineCalculationCGI.exe).

The saturated pressure of H_2SO_4 was measured by Stull (1947) at 420–580 K, Ayers et al. (1980) at 338–445 K, and Richardson et al. (1986) at 263–303 K. According to Ayers et al. (1980),

$$\ln p_{s1}(\text{bar}) = 16.259 - \frac{10156}{T} + 7.08\left(1 + \ln\frac{T_0}{T} - \frac{T_0}{T}\right) \quad (4)$$

The last term is a correction suggested by Kulmala and Laaksonen (1990); they used $T_0 = 360$ K. The observations by Richardson et al. (1986) of H_2SO_4 vapor over sulfuric acid with concentration of 98.479% were corrected to the pure sulfuric acid in Paper 2:

$$\ln p_{s1}(\text{bar}) = 14.07 - 9317/T \quad (5)$$

Both relationships for the saturated H_2SO_4 vapor are shown in Fig. 1 in the temperature range of 200–400 K. They are almost similar in the range of the measurements by Ayers et al. (1980), while the difference is a factor of 3.5 at 270 K, in the range of the measurements by Richardson et al. (1986). The H_2SO_4 vapor pressure is smaller at 263 K than that at 338 K by a factor of 2600 and required a more sophisticated technique in the measurements by Richardson et al. (1986). Therefore relationship (5) looks preferable and will be used in our work.

2.2. Lower cloud boundary

Early models (Krasnopolsky and Parshev, 1981, 1983; Yung and DeMore, 1982) predicted the photochemical production of H_2SO_4 in a thin layer of 2 km centered at 62 km. Paper I favored the column production rate of 2.2×10^{12} cm^{-2} s^{-1} for a model with 30 ppm of H_2O in the lower atmosphere. However, recent photochemical models for the middle atmosphere (Krasnopolsky, 2012; Zhang et al., 2012) predict almost similar H_2SO_4 production rates of 5.7×10^{11} cm^{-2} s^{-1} with peaks at 66 and 64 km,

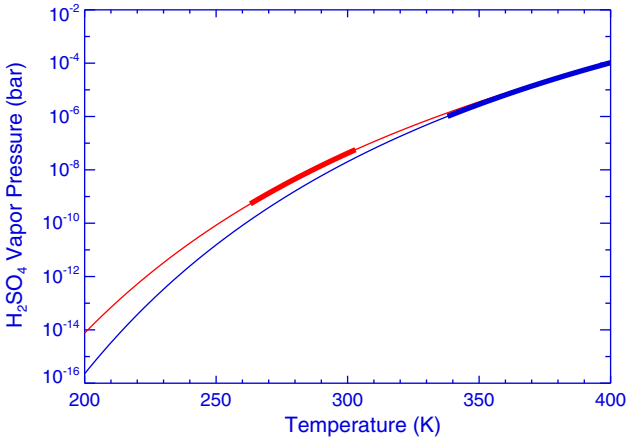

Fig. 1. Saturated vapor pressure over the pure sulfuric acid from the measurements by Ayers et al. (1980) with modification by Kulmala and Laaksonen (1990) (blue) and from Richardson et al. (1986) with adjustment by Krasnopolsky (2011) (red). The thicker parts of the curves indicate the temperature ranges for which the measurements were done. (For interpretation of the references to color in this figure legend, the reader is referred to the web version of this article.)

respectively. The production rate profile from Krasnopolsky (2012) is shown in Fig. 2 and will be used in this work. Profiles of temperature and eddy diffusion (Fig. 3) are taken from the Venus International Reference Atmosphere (VIRA, Seiff et al., 1985) for latitudes of 45°, 60° and from Krasnopolsky (2012), respectively. We will change eddy diffusion below 54 km in our model.

Ground-based (Pollack et al., 1993; de Bergh et al., 1995; Chamberlain et al., 2013; Arney et al., 2014), VEX/SPICAV-IR (Bézard et al., 2011), and VEX/VIRTIS (Marcq et al., 2008; Haus and Arnold, 2010; Tsang et al., 2010) observations result in an H_2O abundance of 30 ppm in the lower atmosphere, and we adopt this value.

According to Paper 2, deviations from the phase equilibrium between the H_2O and H_2SO_4 vapors and the sulfuric acid aerosol begin only above 90 km, and we may safely adopt the phase equilibrium in the much denser and warmer atmosphere below 75 km in this work.

Our method to determine altitude of the lower cloud boundary (LCB) is similar to that in Paper 1. According to the chemical kinetic model for the lower atmosphere of Venus (Krasnopolsky, 2013), the H_2SO_4 vapor mixing ratio is 3.8 ppm at 47 km for the adopted values of the H_2SO_4 flux, eddy diffusion, and temperature. With this boundary condition, the H_2SO_4 vapor mixing ratio f_1 is easily calculated (the blue[1] curve in Fig. 4a) using

$$\Phi_1 = -Kn(z)\frac{df_1}{dz} \quad (6)$$

and assuming that condensation does not occur; n is the total number density. Taking into account the element (hydrogen) conservation (Krasnopolsky, 1995), the lack of condensation and significant quantities of other hydrogen-bearing species, the sum of the H_2O and H_2SO_4 mixing ratios should be constant, and the H_2O mixing ratio is $f_0 = 30$ ppm $- f_1$ (green curve) for the water abundance of 30 ppm in the lower atmosphere. Both f_0 and f_1 curves are actually valid below the LCB that we are trying to find. The next step is to calculate $m = H_2O/H_2SO_4$ in the sulfuric acid clouds (the black curve in Fig. 4a) that corresponds to the obtained H_2O mixing ratio using relationships (1), (3), and the chemical potentials from Giauque

[1] For interpretation of color in Fig. 4, the reader is referred to the web version of this article.

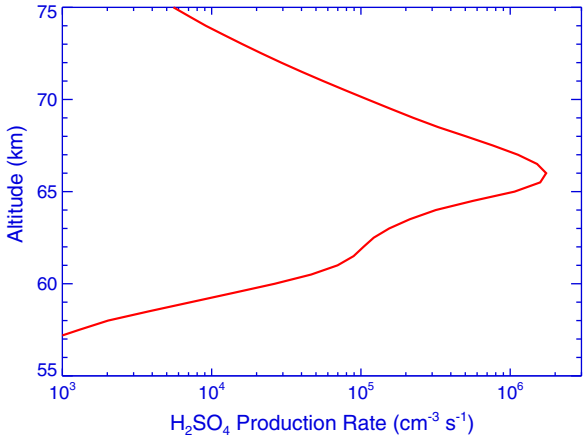

Fig. 2. Vertical profile of the sulfuric acid production rate. The column rate is equal to 5.7×10^{11} cm^{-2} s^{-1}. From Krasnopolsky (2012).

et al. (1960). Then an H_2SO_4 vapor mixing ratio is calculated using m, (1), (5), and Giauque et al. (1960). It is shown by the red curve in Fig. 4a. Intersection of the red and blue curves for H_2SO_4 gives a position of LCB which is at 49 km. The H_2SO_4 vapor is not saturated below this altitude, and liquid sulfuric acid cannot exist for this combination of the H_2SO_4 and H_2O abundances.

Similar calculations for the H_2SO_4 flux that is twice the nominal value of 5.7×10^{11} cm^{-2} s^{-1} are shown in Fig. 4b. The increase of the flux by a factor of 2 in Fig. 4b results in 7.6 ppm of H_2SO_4 at 47 km and moves the LCB from 49 km to 47.4 km. The same effect may be obtained by reduction of eddy diffusion by a factor of 2, because the solution of (6) and all subsequent operations are sensitive to the Φ_1/K ratio.

2.3. Vertical profiles of H_2O, H_2SO_4, and sulfuric acid concentration in the cloud layer

The calculated profiles of H_2O and H_2SO_4 vapors in Fig. 4 become invalid above the LCB. Following Paper I, we will consider now diffusion of the two species in equilibrium with liquid sulfuric acid. For particles with radii exceeding 0.1 μm effects of surface tension on the saturated vapor abundances are negligible, and all particles at a given altitude have the same $m(z) = H_2O/H_2SO_4$. Therefore we may consider a mean mass sedimentation velocity $V(z)$, though true particle velocities for various radii at a given altitude may differ by orders of magnitude. Thus, we have a system with five unknown functions of height: mixing ratios f_0 and f_1 of the H_2O and H_2SO_4 vapors, respectively, number densities n_0 and n_1 of H_2O and H_2SO_4 in the aerosol, respectively, and the mean sedimentation velocity V. Continuity equations for H_2O and H_2SO_4 account for species in both gas and liquid phases:

$$\Phi_0 = -Kn\frac{df_0}{dz} - n_0 V \tag{7}$$

$$\Phi_1 = -Kn\frac{df_1}{dz} - n_1 V \tag{8}$$

However, $\Phi_0 + \Phi_1 = 0$ because of the element (hydrogen) conservation. Escape of H on Venus is weaker than Φ_0, Φ_1 by a few orders of magnitude and may be neglected in our problem. Therefore one gets

$$Kn\left(\frac{df_1}{dz} + \frac{df_0}{dz}\right) = -n_1 V(1+m) \tag{9}$$

Substitution of $n_1 V$ from (9) to (8) gives

$$\Phi_1 = \frac{Kn}{1+m}\left(\frac{df_0}{dz} - m\frac{df_1}{dz}\right) \tag{10}$$

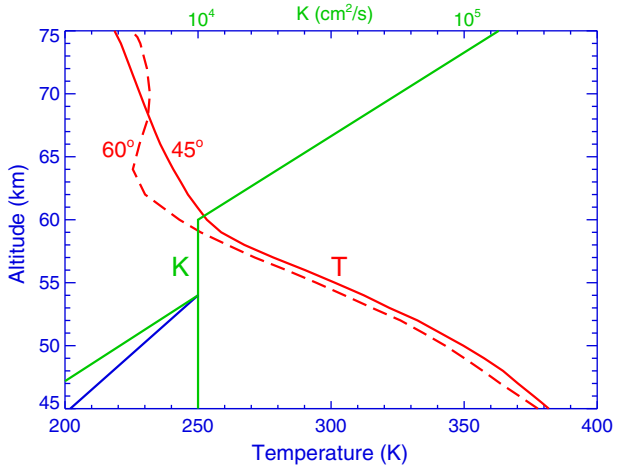

Fig. 3. Profiles of temperature (from VIRA, Seiff et al. (1985)) and eddy diffusion K (from Krasnopolsky (2012)). Maximal and best-fit (blue) changes in eddy diffusion (see Fig. 5) are shown as well. (For interpretation of the references to color in this figure legend, the reader is referred to the web version of this article.)

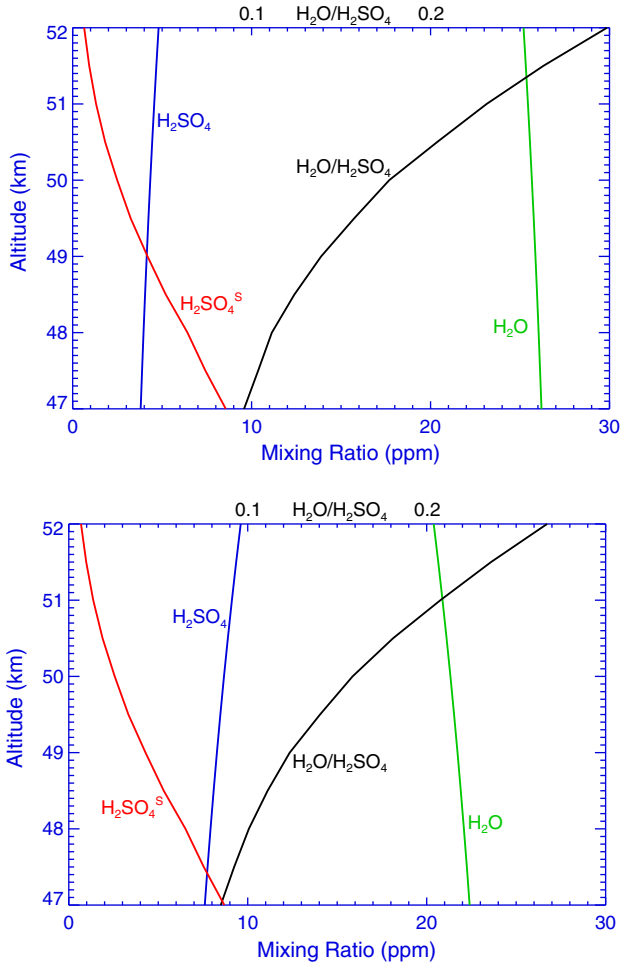

Fig. 4. Determination of LCB for the nominal flux and twice the nominal flux of H_2SO_4 (upper and lower panels, respectively).

The flux of sulfuric acid is equal to

$$\Phi(z) = \Phi_1 = -\int_z^\infty P(x)dx \tag{11}$$

where $P(z)$ is the H_2SO_4 production rate from Fig. 2. The flux is downward and therefore negative.

The H_2O and H_2SO_4 vapor mixing ratios f_0 and f_1 are in equilibrium with sulfuric acid that has concentration

$$C = \frac{1}{1 + m * 18/98} \tag{12}$$

(18 and 98 are the molecular masses of H_2O and H_2SO_4). Therefore we have reduced the system with five unknown functions to Eq. (10) with the only unknown $m(z)$. Values of m, f, and f_0 at the LCB may be found using the method described in Section 2.2 (Fig. 4). Then m is varied at the next altitude, and f_1, f_0 and then Φ are calculated to fit the sulfuric acid flux.

Eq. (10) may be rewritten as

$$m = \frac{Kn\frac{df_0}{dz} - \Phi}{Kn\frac{df_1}{dz} + \Phi} = \frac{n\frac{df_0}{dz} - \frac{\Phi}{K}}{n\frac{df_1}{dz} + \frac{\Phi}{K}} \tag{13}$$

This relationship is more convenient than (10), an adopted m at the next altitude may be compared with the calculated m and varied to get equal values. It is evident from (10) and (13) that the solution depend actually on Φ/K rather than just on the flux Φ.

Changing eddy diffusion with the fixed flux of 5.7×10^{11} cm^{-2} s^{-1}, one may vary LCB. Sum of the H_2O and H_2SO_4 vapor mixing ratios in equilibrium with sulfuric acid has to be equal to 30 ppm at LCB. For example, if LCB is at 47 km with $T = 370$ K, then $m = 0.087$ to fit this condition, and $f_0 = 21.3$ ppm, $f_1 = 8.7$ ppm. The H_2SO_4 vapor mixing ratio is 3.8 ppm for $K_{47} = 10^4$ cm^2 s^{-1} (Section 2.2), and eddy diffusion at LCB = 47 km has to be changed to $10^4 \times 3.8/8.7 = 4370$ cm^2 s^{-1}. We approximate this change by a linear decrease in eddy diffusion below 54 km (Fig. 3). Then vertical profiles of the H_2O and H_2SO_4 vapor mixing ratios and m may be calculated by solving (13) with $m_{47} = 0.087$, $f_0 = 21.3$ ppm, and $f_1 = 8.7$ ppm as the boundary conditions.

Solutions of (13) with adjustments in eddy diffusion below 54 km to fit LCB values of 46–49 km with a step of 0.5 km are shown in Fig. 5. The calculated profiles of H_2SO_4 vapor are identical above LCBs and adopted constant below LCBs because thermal decomposition of H_2SO_4 to SO_3 and H_2O is insignificant above 45 km (Krasnopolsky, 2013). The calculated H_2O profiles look similar but shifted by ~1.3 ppm from each other. This shift is moderate near 50 km, where H_2O varies from 15.6 to 25.3 ppm, but significant above 65 km, where water vapor disappears for LCB ⩽ 46 km.

According to the photochemical model for the middle atmosphere (Krasnopolsky, 2012), almost all production of SO_3 is converted into H_2SO_4, and only ~1% is lost by photolysis and in the reaction with SO. Therefore the production of sulfuric acid (Fig. 2) is almost insensitive to the abundance of water vapor. However, if this abundance becomes extremely low, then the sulfuric acid production becomes smaller, preventing the physically unreasonable solution without H_2O above the clouds.

Calculated variations of sulfuric acid concentration are shown in Fig. 6. The concentration is steeply decreasing from ~98% near LCB to ~80% near 60 km and slightly varies up to 75 km. It is smaller than 85% calculated in Paper 1 at 58–65 km for the H_2SO_4 flux of 2.2×10^{12} cm^{-2} s^{-1} that exceeded our nominal flux by a factor of 4. It is also smaller than 85% at 70–75 km calculated in Paper 2 for high latitudes of 63–88°N, where vertical profiles of H_2O and HDO were observed by the SOIR solar occultations (Fedorova et al., 2008) and temperature profiles were retrieved from the VeRa radio occultations (Tellmann et al., 2009) at 85°N. The observed temperature near 70 km exceeded the VIRA value at 45° used in this paper by 12 K, and this affected the calculated concentration of sulfuric acid.

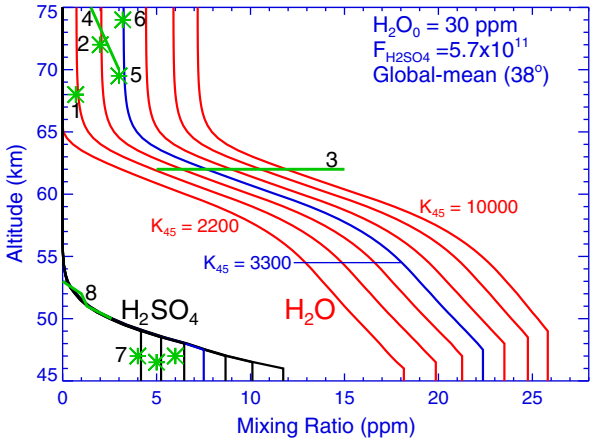

Fig. 5. Vertical profiles of H_2O and H_2SO_4 vapor for the global-mean flux of H_2SO_4 (middle latitudes). Eddy diffusion is adjusted below 54 km (Fig. 3) to fit LCB varying from 46 to 49 km. The preferable profile is show in blue. Observations of H_2O: (1) Fink et al. (1972), (2) KAO (Bjoraker et al., 1992), (3) Venera 15 (Ignatiev et al., 1999), (4) VEX/SOIR occultations (Fedorova et al., 2008), (5) VEX/VIRTIS-H (Cottini et al., 2012), (6) IRTF/CSHELL (Krasnopolsky et al., 2013). Observations of H_2SO_4 vapor: (7) Magellan (Kolodner and Steffes, 1998), (8) VEX/VeRa (Oschlisniok et al., 2012). (For interpretation of the references to color in this figure legend, the reader is referred to the web version of this article.)

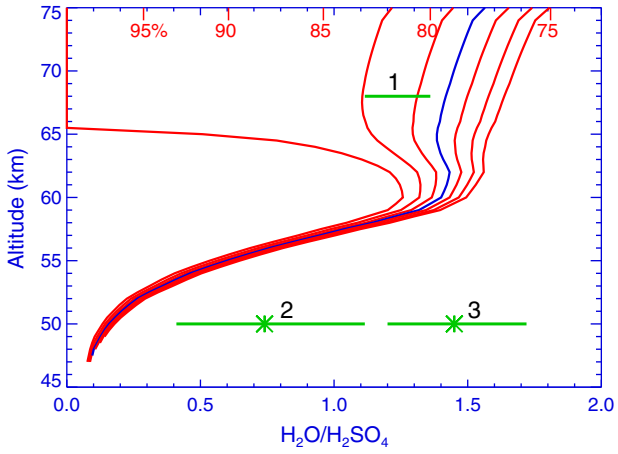

Fig. 6. Variations of $m = H_2O/H_2SO_4$ and concentration in the sulfuric acid droplets. The preferable profile is shown in blue. Observations: (1) VEX/VIRTIS-H (Cottini et al., 2012), (2) VEX/VIRTIS-M (Barstow et al., 2012), (3) ground-based (Arney et al., 2014). (For interpretation of the references to color in this figure legend, the reader is referred to the web version of this article.)

3. Comparison with observations and discussion

To discuss possible variations in the clouds, one has to evaluate typical times of some basic processes (Table 1). The H_2O chemical lifetime is minimal at the peak of sulfuric acid production at 66 km and much longer beyond the peak. Phase equilibrium between vapors of H_2O and H_2SO_4 and droplets of sulfuric acid is almost immediate. All other processes are much slower than the period of the zonal rotation of the atmosphere that varies from 7.5 days at 47 km to 4.5 days at 65 km (VIRA, Kerzhanovich and Limaye, 1985). Therefore variations of the atmospheric properties in the cloud layer with local time are expected to be low.

The times in Table 1 are significantly longer than typical times of ~10 h for features in the middle and lower cloud layers

Table 1
Some characteristic times in the Venus clouds.

Vertical mixing time H^2/K (55 km)	1.5 years
Stokes precipitation (mode 2, r = 1.1 μm, 66–57 km)	0.8 years
Stokes precipitation (mode 3, r = 3.7 μm, 57–47 km)	1 month
Chemical lifetime of H_2O at 66 km (peak of H_2SO_4 production)	1 month

(McGouldrick et al., 2008) that were observed in the transparency windows on the Venus night side using VIRTIS at Venus Express. On the other hand, each of the Vega 1 and 2 balloons (Sagdeev et al., 1986) monitored the middle cloud layer *in situ* at 53 km for 45 h and revealed very uniform clouds during those flights. Anyway, we will not consider variations of the atmospheric properties with local time.

The solar flux at the equator is higher than the global-mean value by a factor of $4/\pi = 1.27$; that at latitude of 60° is equal to $2/\pi = 0.64$ of the global-mean value. The global-mean conditions reflect middle latitudes and actually refer to 38°. We will apply our global-mean model in Figs. 5 and 6 to the low latitudes and to ~60° with the fluxes of H_2SO_4 of 1.2 and 0.7 times the nominal flux, respectively. The results are shown in Figs. 7 and 8.

To change the LCB from 49 to 46 km for the global-mean conditions in Figs. 5 and 6, eddy diffusion at 45 km should be reduced from 10^4 to 2200 $cm^2\ s^{-1}$. The calculated H_2O profiles are compared with aircraft (Fink et al., 1972; Bjoraker et al., 1992), Venera 15 (Ignatiev et al., 1999), VEX/VIRTIS (Cottini et al., 2012), and ground-based (Krasnopolsky et al., 2013) observations. Vertical profiles of H_2O mixing ratio from the VEX/SOIR solar occultations (Fedorova et al., 2008) were observed at 63–88°N and extend to 70 km with mean values decreasing from ~3 ppm at 70 km to ~1.5 ppm at 75 km.

A preferable case with the H_2O mixing ratio of ~3 ppm near 70 km (Cottini et al., 2012; Krasnopolsky et al., 2013) is shown in blue. It corresponds to LCB at 47.5 km and requires reduction of eddy diffusion from 54 to 45 km by a factor of 3.

Nephelometers at the Pioneer Venus entry probes (Ragent and Blamont, 1980) resulted in the mean LCB at 48.4 ± 1.5 km, those at the Venera 9-14 probes showed 49.3 ± 1.2 km, and spectrophotometers at the same probes gave 48.7 ± 1.0 km (Golovin et al., 1981; Moshkin et al., 1983). Three profiles of H_2SO_4 vapor mixing ratio measured by the Magellan radio occultations (Kolodner and Steffes, 1998) showed peaks at 46.5–47 km (Fig. 5). Those peaks indicate LCBs. VIRA (Ragent et al., 1985) gives the LCB at 47.5 km, similar to our preferable value.

Profiles of H_2SO_4 mixing ratio above 50 km were observed by the VeRa radio occultations of Venus Express (Oschlisniok et al., 2012). The mean profile for low and middle latitudes is shown in Fig. 5 and is identical to those from our model.

While H_2O varies near 50 km by a factor of 1.6 in Fig. 5, differences in sulfuric acid concentration between the curves in Fig. 6 are low near 50 km, and even smaller are the variations of H_2SO_4.

The ratio $m = H_2O/H_2SO_4$ in sulfuric acid steeply increases from ~0.15 (98%) at 50 km to ~1.4 (80%) at 60 km with some variations above 60 km (Fig. 6). Our preferable profile has $m \approx 1.5$ (79%) near 70 km. Cottini et al. (2012) found that the H_2O abundances from the VEX/VIRTIS observations correspond to a concentration of 80–83% at 68 km, which is close to our preferable value.

Concentration of sulfuric acid in the Venus clouds is measured using some differences in the spectra of sulfuric acid with concentrations of 75%, 85%, and 96% observed by Palmer and Williams (1975). VEX/VIRTIS (Barstow et al., 2012) and ground-based (Arney et al., 2014) observation in the windows at 1.74 and 2.3 μm probe the lower cloud layer and give the sulfuric acid concentration in that layer. The results are rather different, 88 ± 5% and 79 ± 3%, respectively, at middle latitudes (Fig. 6).

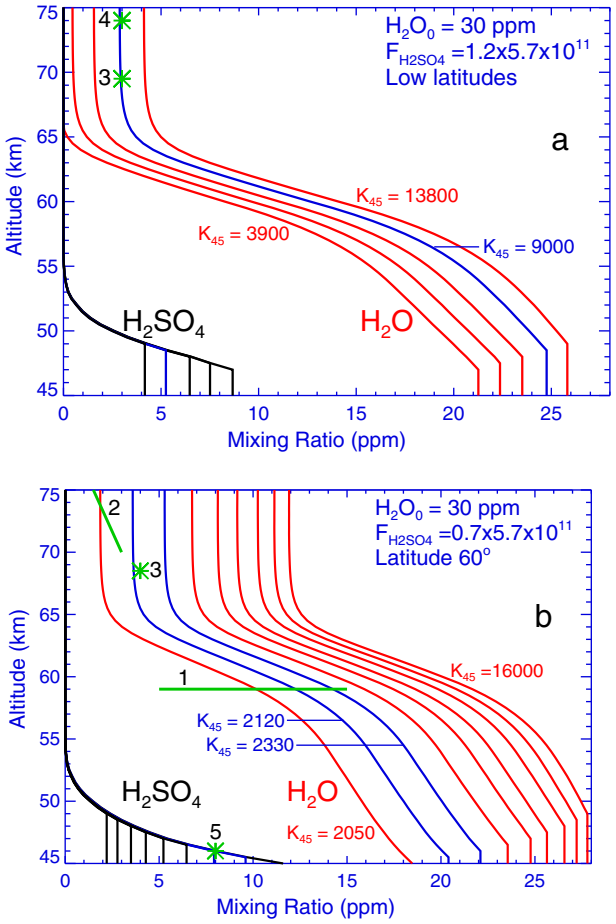

Fig. 7. Vertical profiles of H_2O and H_2SO_4 for conditions typical of the low latitudes and ~60° (upper (a) and lower (b) panels, respectively). The preferable profiles are shown in blue. Observations: (1) Venera 15 (Ignatiev et al., 1999), (2) VEX/SOIR occultations (Fedorova et al., 2008), (3) VEX/VIRTIS-H (Cottini et al., 2012), (4) IRTF/CSHELL (Krasnopolsky et al., 2013), and (5) the VLA observation of H_2SO_4 at high latitudes (Jenkins et al., 2002). (For interpretation of the references to color in this figure legend, the reader is referred to the web version of this article.)

Abundances of water vapor for various concentration of sulfuric acid may be calculated using relationships (1–3) and the chemical potentials from Giauque et al. (1960). The results are shown in Fig. 9. For example, the concentrations of 79% and 88% from Arney et al. (2014) and Barstow et al. (2012) result in f_{H2O} = 5000 ppm and 600 ppm at 50 km, respectively, while the preferable model in Fig. 5 gives 21 ppm.

Calculated profiles of H_2O and H_2SO_4 for low latitudes, where the sulfuric acid production is greater than the global-mean value by a factor of 1.2, are shown in Fig. 7a. The observed H_2O at the low latitudes remains at 3 ppm near 70 km in Cottini et al. (2012) and Krasnopolsky et al. (2013), and the preferable version has LCB at 48.5 km with a minor (by a factor of 1.1) reduction of eddy diffusion to 45 km relative to the value at 54 km. Profiles of sulfuric acid concentration for the low latitudes are shown in Fig. 8a. The concentration is 79% near 70 km for the preferable profile, similar to that for the middle latitudes (Fig. 6).

Our model for latitude of 60° with a decrease in the production of sulfuric acid by a factor of 0.7 is shown in Figs. 7b and 8b. Cottini et al. (2012) indicate an increase in water vapor near 60° from ~3 ppm to ~4 ppm, and two blue curves in the figures fit these abundances. Positions of LCB are at 45.5 and 46 km for these curves, and the H_2SO_4 vapor mixing ratios are 9.5 and 8 ppm, respectively, higher than 4–6 ppm in the Magellan data of

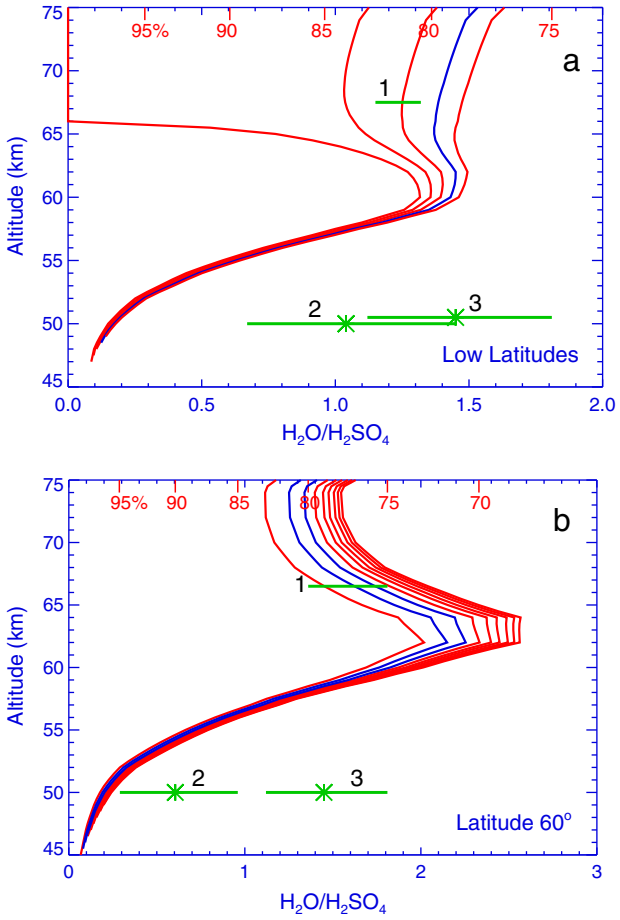

Fig. 8. Vertical profiles of the H_2O/H_2SO_4 ratio and sulfuric acid concentration for conditions typical of the low latitudes and ~60° (upper (a) and lower (b) panels, respectively). The preferable profiles are shown in blue. Observations: (1) Cottini et al. (2012), (2) Barstow et al. (2012), and (3) Arney et al. (2014). (2) and (3) overlap at low latitudes and therefore are slightly shifted vertically. (For interpretation of the references to color in this figure legend, the reader is referred to the web version of this article.)

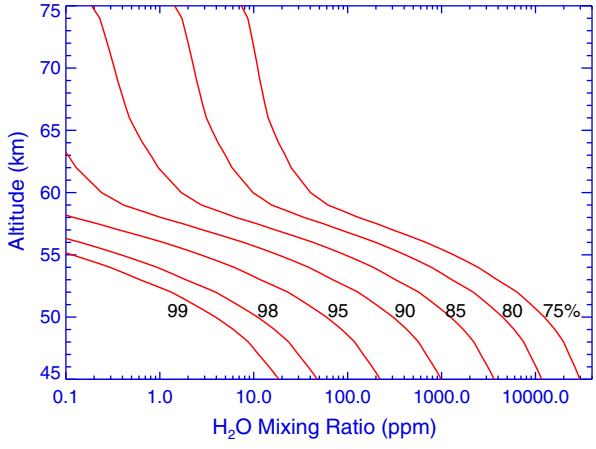

Fig. 9. Abundances of water vapor for various concentration of sulfuric acid.

Kolodner and Steffes (1998) but close to that derived by them for the Mariner 10 radio occultation. The Very Large Array observation by Jenkins et al. (2002) revealed an H_2SO_4 profile with a peak of 8 ppm at 46 km at high latitudes. This peak agrees with our model. The required reduction in eddy diffusion to 45 km is a factor of 4.5

Table 2
Summary of the model basic results.

Parameter	Low latitudes	Middle latitudes (global-mean, 38°)	60°
Φ_{H2SO4} ($cm^{-2}\ s^{-1}$)	$1.2 \times 5.7 \times 10^{11}$	5.7×10^{11}	$0.7 \times 5.7 \times 10^{11}$
$K_{45\ km}$ ($cm^2\ s^{-1}$)	9000	3300	2200
LCB (km)	48.5	47.5	46
H_2SO_4 peak (ppm)	5	7.5	8.5
H_2O at 62 km (ppm)	8	7.5	9
H_2O at 70 km (ppm)	3	3.5	4.5
Concentration at 50 km	98%	98%	98%
60 km	80%	80%	73% at 63 km
70 km	79%	79%	80%

relative to the value at 54 km. The sulfuric acid concentration is 80% near 70 km (Fig. 8b).

Summary of the model basic results is given in Table 2. Our model fits the observed constant H_2O mixing ratio of 3 ppm from the equator to 50° (Cottini et al., 2012; Krasnopolsky et al., 2013) with an increase to 3.5–5 ppm at 60° for eddy diffusion at 45 km decreasing from 9000 to 3300 and then 2200 $cm^2\ s^{-1}$ at the low and middle latitudes and then 60°, respectively. The higher heating at the low latitudes may stimulate higher eddy diffusion there. Generally, features of the Hadley circulation are involved here but cannot be accounted quantitatively by our one-dimensional model. The upward flow at the low latitudes should raise the upper cloud boundary and expose enrichment in water vapor. However, both effects are compensating and rather smooth in the observations, including those from Venera 15 (Zasova et al., 2006; Ignatiev et al., 1999). A decline in the upper cloud boundary to 60° by ~2 km was observed by Venera 15 and Venus Express (Zasova et al., 2006; Cottini et al., 2012). It looks like this decline explains the observed enrichment in water vapor, though the downwelling air is depleted in water.

Variations of eddy diffusion in the lower cloud layer within a factor of 5 induce variations of the LCB from 45 to 49 km, the H_2SO_4 peak abundance from 2 to 11 ppm, and water vapor near LCB from 18 to 28 ppm. However, the most dramatic variations are in water vapor at 65–75 km, which varies up to 12 ppm. While very high sensitivity of the water abundance near the cloud tops to minor variations in eddy diffusion was discussed in the early model by Krasnopolsky and Parshev (1981, 1983) and later confirmed in Krasnopolsky (2012), this fact looks intuitively unexpected.

H_2O and H_2SO_4 abundances are sensitive to small variations of temperature (see Section 2.1). We use two temperature profiles from VIRA (Fig. 3) in this work. Any temperature perturbations should induce perturbations in H_2O and H_2SO_4 abundances as well.

4. Conclusions

This work is an update of the method developed by Krasnopolsky and Pollack (1994) to model vertical profiles of H_2O and H_2SO_4 vapors and sulfuric acid concentration in the Venus cloud layer. Improved thermodynamic parameters for H_2O and H_2SO_4 are used, and the photochemical production of sulfuric acid is significantly reduced to fit the current models. The model is applied to the global-mean conditions and those at the low latitudes and at 60°. Variations in eddy diffusion near the lower cloud boundary are used to simulate atmospheric dynamics that results variability in the cloud properties and abundances of H_2O and H_2SO_4.

The best version of the model for the global-mean condition gives LCB at 47.5 km, H_2SO_4 peak abundance of 7.5 ppm at the LCB, and H_2O mixing ratios of 7 ppm at 62 km and 3.5 ppm above

67 km. The model for low latitudes results in LCB at 48.5 km, the H_2SO_4 peak of 5 ppm, H_2O of 8.5 ppm at 62 km and 3 ppm above 67 km. The model for 60° shows LCB at 46 km, the H_2SO_4 peak of 8.5 ppm, H_2O of 9 ppm at 62 km and 4.5 ppm above 67 km. The calculated variability is induced by the proper changes in the production of sulfuric acid (by factors of 1.2 and 0.7 for the low latitudes and 60°, respectively) and reduction of eddy diffusion near 45 km by factors of 1.1, 3, and 4.5 relative to the value at 54 km for the low and middle (global-mean) latitudes and 60°, respectively. Concentration of sulfuric acid at the low and middle latitudes varies from 98% near 50 km to ~80% at 60 km and then almost constant at 79% at 70 km. Concentration at 60° is 98% at 50 km, 73% at 63 km, and 81% at 70 km. There is a reasonable agreement between the model results and observations except for the sulfuric acid concentration in the lower cloud layer. Variations of eddy diffusion in the lower cloud layer simulate variations in atmospheric dynamics and induce strong variations in water near the cloud tops. Variations in temperature may affect abundances of the H_2O and H_2SO_4 vapors as well.

Acknowledgment

This work is supported by Grant 11.G34.31.0074 of the Russian Government to Moscow Institute of Physics and Technology (Phys-Tech) and V.A. Krasnopolsky.

References

Arney, G. et al., 2014. Spatially resolved measurements of H_2O, HCl, CO, OCS, SO_2, cloud opacity, and acid concentration in the Venus near-infrared spectral windows. J. Geophys. Res. (Planets) 119, 1860–1891.
Ayers, G.P., Gillett, R.W., Gras, J.L., 1980. On the vapor pressure of sulfuric acid. Geophys. Res. Lett. 7, 433–436.
Barstow, J.K. et al., 2012. Models of the global cloud structure on Venus derived from Venus Express observations. Icarus 217, 542–560.
Bézard, B. et al., 2011. The 1.10- and 1.18-μm nightside windows of Venus observed by SPICAV-IR aboard Venus Express. Icarus 216, 173–183.
Bjoraker, G.L. et al., 1992. Airborne observations of the gas composition of Venus above the cloud tops: Measurements of H_2O, HDO, HF and the D/H and $^{18}O/^{16}O$ isotope ratios. Bull. Am. Astron. Soc. 24, 995 (abstract).
Chamberlain, S. et al., 2013. Ground-based near-infrared observations of water vapour in the Venus troposphere. Icarus 222 (1), 364–378.
Cottini, V. et al., 2012. Water vapor near the cloud tops of Venus from Venus Express/VIRTIS dayside data. Icarus 217, 561–569.
De Bergh, C. et al., 1995. Water in the deep atmosphere of Venus from high-resolution spectra of the night side. Adv. Space Res. 15 (4), 79–88.
Fedorova, A. et al., 2008. HDO and H_2O vertical distributions and isotopic ratio in the Venus mesosphere by solar occultation at infrared spectrometer on board Venus Express. J. Geophys. Res. 113, E00B22.
Fink, U. et al., 1972. Water vapor in the atmosphere of Venus. Icarus 17, 617–631.
Gao, P. et al., 2014. Bimodal distribution of sulfuric acid aerosol in the upper haze of Venus. Icarus 231, 83–98.
Giauque, W.F. et al., 1960. The thermodynamic properties of aqueous sulfuric acid solutions and hydrates from 15 to 300 K. J. Am. Chem. Soc. 82, 62–67.
Golovin, Yu.M., Moshkin, B.E., Ekonomov, A.P., 1981. Aerosol component properties as measured by the Venera 11 and 12 spectrophotometer. Cosmic Res. 19, 295–302.
Haus, R., Arnold, G., 2010. Radiative transfer in the atmosphere of Venus and application to surface emissivity retrieval from VIRTIS/VEX measurements. Planet. Space Sci. 58 (12), 1578–1598.
Ignatiev, N.I. et al., 1999. Water vapor in the middle atmosphere of Venus: An improved treatment of the Venera 15 IR spectra. Planet. Space Sci. 47, 1061–1075.
Jenkins, J.M. et al., 2002. Microwave remote sensing of the temperature and distribution of sulfur compounds in the lower atmosphere of Venus. Icarus 158, 312–328.
Kerzhanovich, V.V., Limaye, S.S., 1985. Circulation of the atmosphere from the surface to 100 km. Adv. Space Res. 5 (#11), 59–84.
Kolodner, M.A., Steffes, P.G., 1998. The microwave absorption and abundance of sulfuric acid vapor in the Venus atmosphere based on new laboratory measurements. Icarus 132, 151–169.
Krasnopolsky, V.A., 1995. Uniqueness of a solution of a steady-state photochemical problem: Applications to Mars. J. Geophys. Res. 100, 3263–3276.
Krasnopolsky, V.A., 2011. Vertical profile of H_2SO_4 vapor at 70–110 km and some related problems. Icarus 215, 197–203 (Paper 2).
Krasnopolsky, V.A., 2012. A photochemical model for the Venus atmosphere at 47–112 km. Icarus 218, 230–246.
Krasnopolsky, V.A., 2013. S_3 and S_4 abundances and improved chemical kinetic model for the lower atmosphere of Venus. Icarus 225, 570–580.
Krasnopolsky, V.A., Parshev, V.A., 1981. Chemical composition of the atmosphere of Venus. Nature 292, 610–613.
Krasnopolsky, V.A., Parshev, V.A., 1983. Photochemistry of the Venus atmosphere. In: Hunten, D.M., Colin, L., Donahue, T.M., Moroz, V.I. (Eds.), Venus. Univ. Arizona Press, Tucson, pp. 431–458.
Krasnopolsky, V.A., Pollack, J.B., 1994. H_2O–H_2SO_4 system in Venus' clouds and OCS, CO, and H_2SO_4 profiles in Venus' troposphere. Icarus 109, 58–78 (Paper 1).
Krasnopolsky, V.A. et al., 2013. Observations of D/H ratios in H_2O, HCl, and Hf on Venus and new DCl and DF line strengths. Icarus 224, 57–65.
Kulmala, M., Laaksonen, A., 1990. Binary nucleation of water–sulfuric acid system: Comparison of classical theories with different H_2SO_4 saturation vapor pressure. J. Chem. Phys. 93, 696–701.
Marcq, E. et al., 2008. A latitudinal survey of CO, OCS, H_2O, and SO_2 in the lower atmosphere of Venus: Spectroscopic studies using VIRTIS-H. J. Geophys. Res. 113, E00B07. http://dx.doi.org/10.1029/2008JE003074.
McGouldrick, K. et al., 2008. Venus Express/VIRTIS observations of middle and lower cloud variability and implications for dynamics. J. Geophys. Res. 113, E00B14.
Mills, F.P., Allen, M., 2007. A review of selected issues concerning the chemistry in Venus' middle atmosphere. Planet. Space Sci. 55, 1729–1740.
Moshkin, B.E. et al., 1983. Veneras 13 and 14 spectrophotometric experiment. I. Methodics, results, and preliminary analysis of measurements. Cosmic Res. 21, 177–186.
Murphy, D.M., Koop, T., 2005. Review of the vapour pressures of ice and supercooled water for atmospheric applications. Quart. J. Roy. Meteorol. Soc. 131, 1539–1565.
Oschlisniok, J. et al., 2012. Microwave absorptivity by sulfuric acid in the Venus atmosphere: First results from the Venus Express Radio Science experiment VeRa. Icarus 221, 940–948.
Palmer, K.F., Williams, D., 1975. Optical constants of sulfuric acid: Applications to the cloud of Venus? Appl. Opt. 14, 208–219.
Pollack, J. et al., 1993. Near-infrared light from Venus' nightside: A spectroscopic analysis. Icarus 103, 1–42.
Ragent, B., Blamont, J.E., 1980. The structure of the clouds of Venus: Results of the Pioneer Venus nephelometer experiment. J. Geophys. Res. 85, 8089–8105.
Ragent, B. et al., 1985. Particulate matter in the Venus atmosphere. Adv. Space Res. 5 (#11), 85–115.
Richardson, C.B., Hightower, R.L., Pigg, A.L., 1986. Optical measurement of the evaporation of sulfuric acid droplets. Appl. Opt. 25, 1226–1229.
Sagdeev, R.Z. et al., 1986. Overview of Vega Venus balloon in situ meteorological measurements. Science 231, 1411–1414.
Seiff, A. et al., 1985. Models of the structure of the atmosphere of Venus from the surface to 100 km altitude. Adv. Space Res. 5 (11), 3–58.
Stull, D.R., 1947. Vapor pressure of pure substances—Inorganic compounds. Ind. Eng. Chem. 39, 540–550.
Tellmann, S. et al., 2009. Structure of the Venus neutral atmosphere as observed by the Radio Science experiment VeRa on Venus Express. J. Geophys. Res. 114, E00B36.
Tsang, C.C.C. et al., 2010. Correlations between cloud thickness and sub-cloud water abundance on Venus. Geophys. Res. Lett. 37, L02202.
Yung, Y.L., DeMore, W.B., 1982. Photochemistry of the stratosphere of Venus: Implications for atmospheric evolution. Icarus 51, 199–247.
Zasova, L.V. et al., 2006. Structure of the venusian atmosphere from surface up to 100 km. Cosmic Res. 44, 364–383.
Zhang, X. et al., 2012. Sulfur chemistry in the middle atmosphere of Venus. Icarus 217, 714–739.